Biol. Cybern. 69, 57–66 (1993)

Biological Cybernetics

Dynamics of the olfactory bulb: bifurcations, learning, and memory

P. Érdi [1,2], T. Grőbler [1,2], G. Barna [1,3], K. Kaski [2]

[1] Biophysics Group, KFKI Research Institute for Particle and Nuclear Physics of the Hungarian Academy of Sciences, P.O. Box 49, H-1525 Budapest, Hungary
[2] Tampere University of Technology, Microelectronics Laboratory, P.O. Box 527, SF-33101 Tampere, Finland
[3] Department of Artificial Intelligence, Kyushu Institute of Technology, Iizuka 820, Fukuoka, Japan

Received: 22 June 1992/Accepted in revised form: 22 November 1992

Abstract. A mathematical model for describing dynamic phenomena in the olfactory bulb is presented. The nature of attractors and the bifurcation sequences in terms of the lateral connection strength in the mitral layer are studied numerically. Chaotic activity has only been found in the case of strong excitatory coupling. Synaptic modification-induced transition from oscillation to chaos is demonstrated. A model for a simple associative memory is also presented.

1 Introduction

The overwhelming majority of biologically motivated neural models dealing with sensory information processing study the visual system. Recently, however, interest in modelling of the olfactory system, and particularly its first relay station, the olfactory bulb (OB), has arisen and grown (Freeman and Skarda 1985; Baird 1986; Li and Hopfield 1989; Li 1990).

Although many details of the different aspects of olfaction such as the nature of stimuli, mechanism of reception and central processing, olfactory coding, learning and memory have been studied (e.g. Halász 1990; Holley 1991; Scott 1991), we are still far from an understanding of even the fundamental principles of olfactory information processing.

It has been suggested for a long time by the pioneering work of Freeman (1975, 1978) that the spatiotemporal activity patterns of the OB measured by electroencephalogram (EEG) can be interpreted within the framework of dynamic system theory. One important message of Freeman's experimental and theoretical work is that the rhythmic–arrhythmic bulbar activity is the result of the interactions between excitatory (mitral) and inhibitory (granule) cell populations.

Correspondence to: P. Érdi

A few other mathematical models have been previously formulated to explain different aspects of odour coding and bulbar dynamics. The static nature of the projections between the receptor–glomerular and the glomerular–mitral layers, and also of intralayer interactions has been studied (Schild 1988). A structure with specific connectivity and fixed synaptic strengths has been identified (Li and Hopfield 1989; Li 1990) which gives rise to oscillatory activity. The necessity for the unification of models of activity pattern formation, pattern recognition, and associative memory has already been suggested by Baird (1986, 1990). He combined continuous-time activity equations with a "one-shot" learning rule. A simple model for the accessory OB in which the effect of learning is implicitly taken into account has been elaborated by Taylor and Keverne (1991).

To have a coherent view of the dynamics of bulbar information processing, a two-level model was adopted to describe simultaneously both neural activity and synaptic modifiability. The model presented here is based on the Li–Hopfield model, but it takes explicitly into account (1) the lateral interactions in the mitral layer and (2) the modifiability of certain synapses. Three families of problems were studied. In order to gain a clear picture of the dynamic properties of the system, the input was constant over time in the first two families, while the temporal character of the sensory input ("sniff cycle") was explicitly taken into account in the third class of calculations.

First, the effect of lateral connection in the mitral layer was investigated. Because of the lack of firm data on the physiological nature of the lateral interactions in the mitral layer, the potential effects of both inhibition and excitation on the dynamic behaviour were studied. The strengths of the lateral connections were taken to be constant over time, and could be varied through a control parameter. Simulation experiments have shown the occurrence of a series of bifurcation phenomena. It was observed that chaos was only generated when lateral connections were assumed to be excitatory.

Second, the excitatory mitral–mitral interactions were modified by slowly varying the bifurcation

parameter in time. The modification followed the Hebb rule (Hebb 1949), while the activity equations remained unchanged. Adopting a moderately slow learning process, a continuous-time transition from oscillatory to chaotic regime was shown.

Third, the associative character of the OB was demonstrated. In our model (a) odour qualities were coded in spatial amplitude patterns; (b) the representation of the qualities had a distributive character; (c) lower stimulus intensity implied the stimulation of less input cells; (d) sensory inputs were continuous in time; (e) learning was a continuous process, (f) the learning rule was constructed by supplementing the Hebb rule with a non-linear forgetting term and a selective decreasing term. It is important to note that neurobiologically motivated constraints imposed a severe restriction on the form of the activity responses.

A short review of the neurobiological background is given in Sect. 2. The structural and dynamic aspects of the model are described in Sect. 3. Specific problems of pattern formation and pattern recognition are formulated, and the results of simulation experiments are presented in Sect. 4. These results and further problems to be solved are discussed in Sect. 5.

2 Neurobiological background

The olfactory bulb is the first relay centre of the olfactory system. Anatomical, physiological, neurochemical and behavioural studies provide a considerable amount of information on the structure and function of the OB (Scott and Harrison 1986; Halász 1990; Schild 1990; Shepherd and Greer 1990; Holley 1991; Scott 1991).

2.1 Structural aspects

The OB is a highly layered structure, with synaptic contacts between particular neurons precisely localized in individual layers. Cellular elements in the OB are arranged in a series of layers, namely the olfactory nerve, glomerular, external plexiform, mitral cell, internal plexiform and granule cell layers and the periventricular zone. There is a broad topographical projection of the receptor sheet onto the bulbar surface and a strong convergence of receptor axons onto the synaptic transduction sites, the glomeruli.

Four basic cell types can be found in the OB, namely the mitral/tufted, periglomerular, granule and short axon cells. The mitral cells are excitatory and interact with the inhibitory, axonless granule cells ($\approx$200/mitral cell) via their basal dendrites and also via collaterals. Mitral cells receive inputs from the olfactory receptor cells. These inputs undergo several transformations, mainly in the glomeruli, which contribute to the spatial organization of the mitral responses. Since our attention was focused on understanding the implications of the mitral–granule interaction, the details of glomerular compartmentalization (Schild and Riedel 1992) and of inter-glomerular interaction (Scott and Harrison 1987) were not taken into account here. The outgoing fibres of the OB, i.e. the axons of the output (mitral and tufted) cells, constitute the lateral olfactory tract (LOT), connecting the OB and the olfactory cortex. There are some indications for the existence of lateral connections among the mitral cells. These cells are excitatory (Willey 1973), but it cannot be excluded that lateral connections might be inhibitory in consequence of some indirect mechanism.

Granule cells are the main targets of inputs coming from the olfactory cortex and other higher centres. Specifically, the cortical projections form excitatory synapses onto granule cells, and their stimulation leads to the inhibition of mitral cells.

2.2 Functional aspects

Olfaction-induced slow cycles (sniff cycles) were demonstrated by Adrian (1950), and many types of complex dynamic behaviour such as oscillation and chaos have been observed using EEG recordings (e.g. Skarda and Freeman 1987). It was suggested that sensory information was encoded in spatiotemporal periodic and chaotic patterns. Physiologically measured EEG patterns (Freeman 1978; Freeman and Schneider 1982) showed oscillations with the same frequency (35–90 Hz) in different parts of the OB. Although these oscillations only had a minor phase variation, significant differences of amplitude could be found over the bulb.

It has been demonstrated by combining anatomical and behavioural studies (Hudson and Distel 1987) that up to 80% of bulbar tissue can be removed without apparent functional loss.

Learning is a very important aspect of odour coding. Excitatory mitral–mitral synapses (Willey 1973) and/or the reciprocal dendro–dendritic synapses between mitral and granule cells (Brennan and Keverne 1989; Brennan et al. 1990; Trombley and Shepherd 1991) might be modifiable.

3 The model

3.1 Structural aspects

The model consists of two layers of neurons: (1) the layer of excitatory mitral cells, and (2) the layer of inhibitory granule cells. The rather significant difference between the number of cells in these two layers of the OB was neglected and both layers were assumed to contain N units. The model neurons were arranged in a one-dimensional ring (the Nth and the 1st neurons were considered as neighbours) in order to avoid wall effects. A fragment of the network is shown in Fig. 1.

Each unit has an internal state corresponding to the membrane potential of the cell which was converted by a static non-linear transfer function to yield the output of the cell. This output can be interpreted as the firing rate of the cell.

Each mitral cell excites the three nearest granule cells. The physiological nature of lateral connections within the mitral layer is not specified here: both excita-

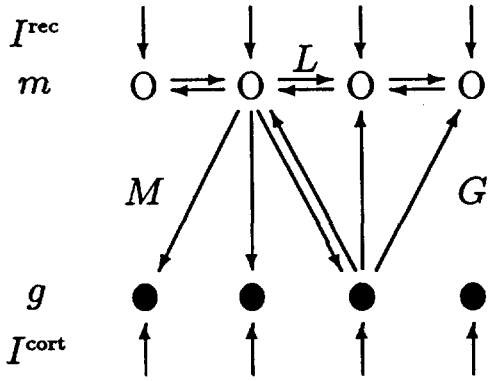

Fig. 1. Model structure of OB. The two layers of excitatory mitral (*m*, *circles*) and inhibitory granule (*g*, *filled circles*) cells interact through the connections M and G. L denotes modifiable lateral connections in the mitral layer

tory and inhibitory connections were investigated and their different effects on the qualitative dynamics of the model are discussed (Sect. 4.1). In these simulations (and also in Sect. 4.2), nearest neighbour connections were studied, while full lateral interconnection was assumed when modelling associative memory (Sect. 4.3).

Granule cells receive constant input corresponding to the modulatory effect of cortical regions and other higher centres. The granule-to-mitral synapses are inhibitory. No lateral connections were assumed in the granule cell layer.

3.2 Activity dynamics

Membrane potentials of mitral and granule cells at time t were expressed by the real vectors $m(t) = \{m_1(t), m_2(t), \ldots, m_N(t)\}$ and $g(t) = \{g_1(t), g_2(t), \ldots, g_N(t)\}$, respectively. Their transfer functions were denoted by ϕ_m and ϕ_g. The form of these functions was taken from Li and Hopfield (1989) in order to be able to compare our results even though the derivative of experimentally measured curves (Freeman 1979) significantly departs from those used by Li and Hopfield.

$$\phi_m(m_i) = \begin{cases} S'_m + S'_m \tanh\left(\dfrac{m_i - \theta}{S'_m}\right) & \text{if } m_i < \theta \\ S'_m + S_m \tanh\left(\dfrac{m_i - \theta}{S_m}\right) & \text{if } m_i \geqslant \theta, \end{cases} \tag{1}$$

$$\phi_g(g_i) = \begin{cases} S'_g + S'_g \tanh\left(\dfrac{g_i - \theta}{S'_g}\right) & \text{if } g_i < \theta \\ S'_g + S_g \tanh\left(\dfrac{g_i - \theta}{S_g}\right) & \text{if } g_i \geqslant \theta, \end{cases}$$

where $S'_m = 0.14$, $S_m = 1.4$, $S'_g = 0.29$, $S_g = 2.9$, and $\theta = 1$.

The time evolution equations governing the activity dynamics were specified by the following set of coupled, non-autonomous, non-linear, first-order ordinary differential equations (ODEs):

$$\dot{m}_i(t) = -a \cdot m_i(t) - b \sum_{j=1}^{N} G_{ij}\phi_g(g_j(t)) + \\ + c \sum_{j=1}^{N} L_{ij}\phi_m(m_j(t)) + I_i^{rec}(t), \tag{2}$$

$$\dot{g}_i(t) = -d \cdot g_i(t) + e \sum_{j=1}^{N} M_{ij}\phi_m(m_j(t)) + I_i^{cort},$$

where $i = 1, 2, \ldots, N$; a, b, d, e are positive constants; and c can be positive or negative depending on whether lateral excitation or lateral inhibition is assumed. The only source of non-linearity is the form of the transfer functions. Non-autonomy is due to the temporal character of the input. The synaptic matrices M, G, L correspond to the mitral-to-granule, granule-to-mitral, and lateral (mitral-to-mitral) connections, respectively. It is argued that the lateral connections are modifiable so L may be a function of time (see Sects. 4.2, 4.3) but M and G are fixed. I^{cort} and $I^{rec}(t)$ denote the cortical and receptor inputs, respectively, and

$$I^{rec}(t) = \alpha I^{odour}(t) + I^{backgr}, \tag{3}$$

where α scales the input intensities. $I^{odour}(t)$ contains information about the quality and intensity of odours, and the background I^{backgr} is assumed to be constant over time.

4 Pattern formation and pattern recognition: some problems

4.1 Bifurcation analysis

Given a model structure and the related set of ODEs, the first question to be answered here is what qualitative dynamical behaviour emerges in the parameter space. The nature of attractors, the parameter windows belonging to them, and the bifurcation sequences need to be determined through systematic (numerical) studies.

4.1.1 Formalization of the problem. To study the inherent bulbar dynamics, the time-dependence of external inputs was omitted here, i.e. $I_i^{odour}(t) = \text{const.}$ for any cell i. While all elements of the modulatory cortical input I^{cort} and the receptor background input I^{backgr} vectors have the same values, odour patterns were taken into account by assigning randomly chosen values to the different elements I_i^{odour}. Then the free parameters in (2) are a, b, c, d, e and the input vectors I^{backgr} and I^{cort}.

Li and Hopfield (1989) did not systematically analyse the effect of lateral connections. Problems concerning the physiological nature of these connections have been discussed in Sects. 2 and 3.1. It was therefore particularly important to study the different – positive and negative – values of the parameter c which controls the sign and strength of lateral connections in the mitral layer while the synaptic matrices were fixed. The main question was which values of the parameter c implied

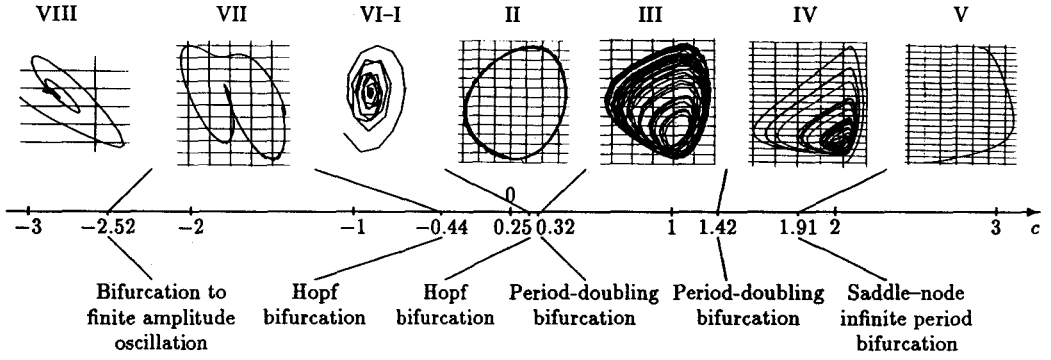

Fig. 2. Attractor regions in terms of the bifurcation parameter c in the range $(-3-3)$. In each region, a characteristic phase diagram is shown. Bifurcation types between the regions are also indicated

stationary, oscillatory or chaotic behaviour and what kinds of bifurcation phenomena could be observed between the different parameter regions. To complete the analysis, experiments with the other parameters were also carried out.

4.1.2 Simulation results. Simulations showed that, for either sign of c, the parameters listed above could be classified into two groups: the systematic change of $|c|$, d and I^{rec} generated the same bifurcation sequence, respectively, although the size of the parameter windows might be different. All these parameters act in the direction of mitral cell excitation (or disinhibition). The change of the other group of parameters, i.e. a, b, e, and I^{cort}, had just the opposite effect (mitral cell inhibition or granule cell excitation) thus the same bifurcation sequence appeared in reversed order. Note that this phenomenon was observed in the case of positive parameter values except for c, which could be either positive or negative.

A bifurcation diagram can be constructed by representing each attractor region in the space of the bifurcation parameters (Borisyuk and Kirillov 1990; Frouzakis et al. 1991). For the above reasons, however, results are presented here only in terms of one parameter, the lateral connection strength c. Values of the other parameters were fixed (see Appendix).

Figure 2 shows the different attractor types with a characteristic phase diagram in each region. The activity of an arbitrary mitral–granule pair was chosen for the two-dimensional representation of phase portraits.

At $c = 0$, the trajectories converged into a stable focus. When lateral excitation was considered ($c > 0$), the following attractor regions of Fig. 2 could be observed as c increased:

Region I: fixed point (stable focus)
Region II: limit cycle
Region III: strange attractor
Region IV: coexistence of limit cycle and strange attractor
Region V: coexistence of fixed point (stable node) and strange attractor

For negative values of c (lateral inhibition), the attractor regions were as follows as $|c|$ increased:

Region VI: fixed point (stable focus)
Region VII: limit cycle
Region VIII: fixed point (stable focus)

These results showed that chaos could only be found when $c > 0$, so, in our model, lateral excitation was necessary to obtain chaotic activity. It was also observed that all neurons oscillate in phase in each periodic region (and also during damping oscillation to a stable focus) and no wave phenomena were detected in the parameter range studied here.

To complete the analysis, not only the nature of the attractors but also the different types of bifurcations between them were identified. At small values of $|c|$, the first bifurcation was a Hopf bifurcation in the case of both lateral excitation and inhibition (between regions I–II and VI–VII in Fig. 2). The fine structure of this type of bifurcation is shown in Fig. 3. At somewhat

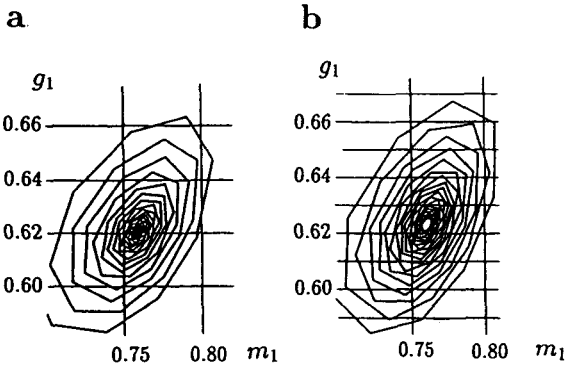

Fig. 3a, b. Typical scheme of Hopf bifurcation. **a** Stable focus with long oscillatory transient at $c = 0.23$; **b** the periodic attractor emerging at $c = 0.25$ with very small amplitude

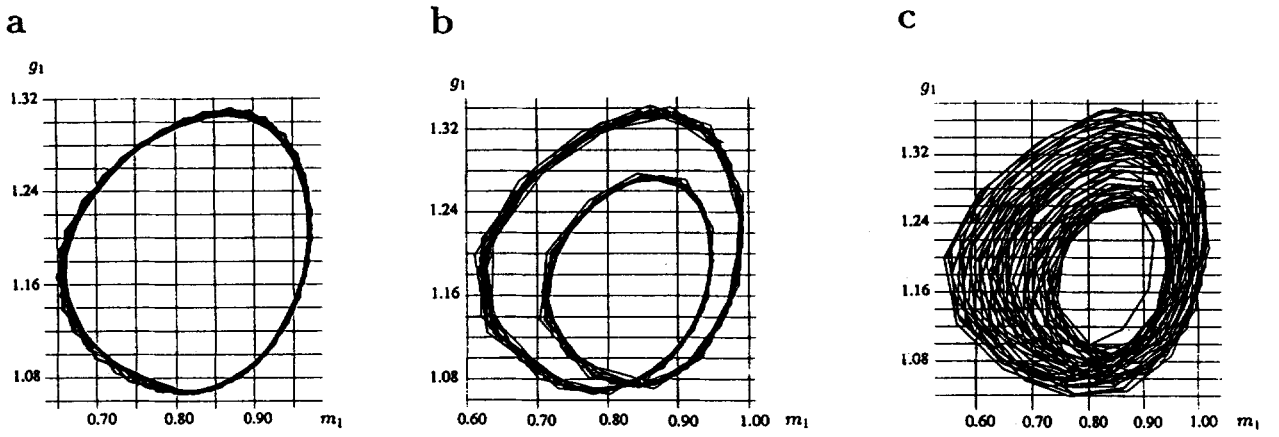

Fig. 4a–c. Period doubling bifurcation. **a** Periodic attractor at $c = 0.3$; **b** biperiodic attractor at $c = 0.32$; **c** strange attractor at $c = 0.34$

larger values of $|c|$, the amplitude of the limit cycle continously increased.

The bifurcation between regions II and III was a period-doubling bifurcation (Fig. 4).

There was a coexistence phenomenon in regions IV and V. While the strange attractor remained stable over the regions III, IV, and V, a stable limit cycle also appeared in region IV. Increasing c further, the period of this limit cycle began to grow and large plateaus appeared (Fig. 5a–d). Finally, as the period of the oscillation became infinitely large (Fig. 5e), the limit cycle disappeared and a stable node emerged. This was characteristic of the so-called saddle-node infinite period bifurcation (Keener 1981).

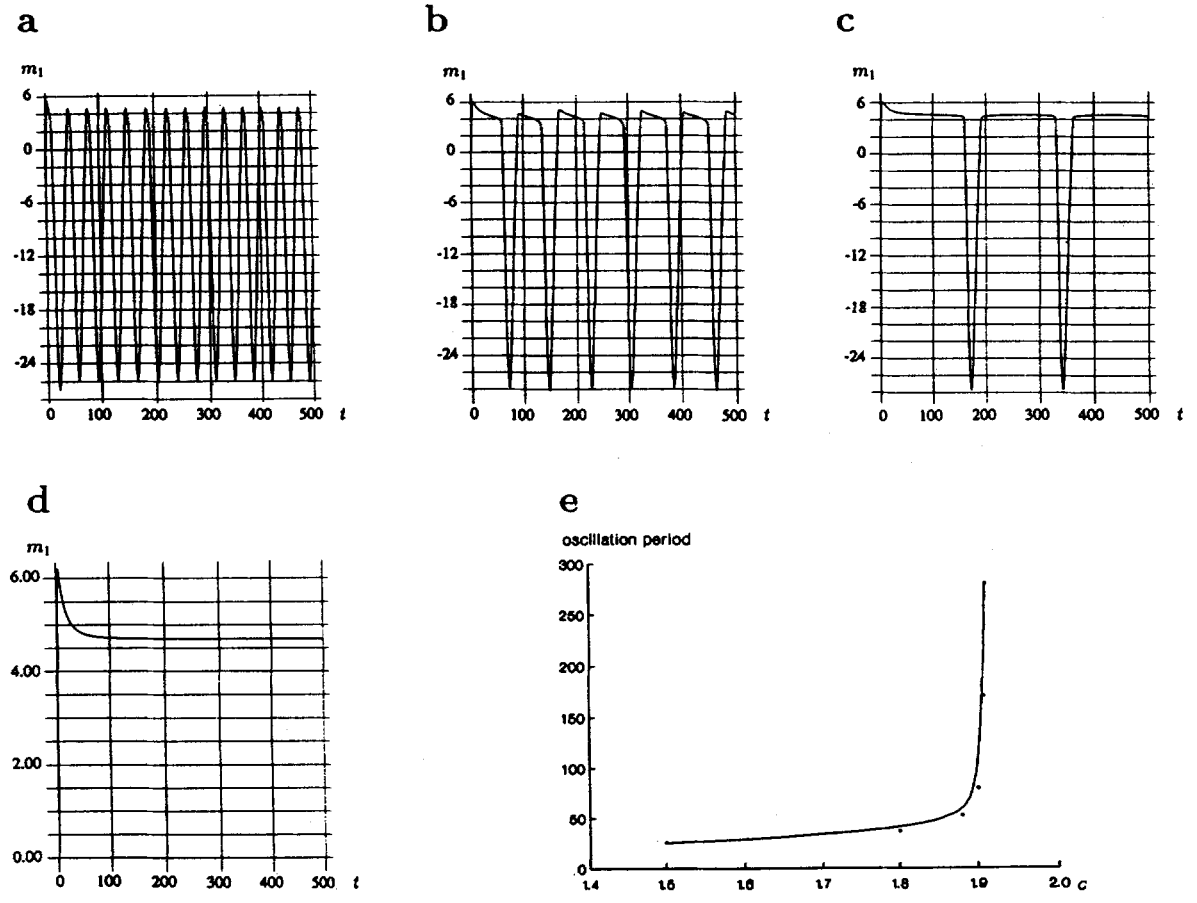

Fig. 5a–e. Saddle-node infinite period bifurcation. Oscillations at **a** $c = 1.80$, **b** $c = 1.90$, **c** $c = 1.908$ and **d** stable node at $c = 1.91$. Time curves instead of phase portraits are plotted directly to visualize period differences. **e** The period of oscillations in terms of the bifurcation parameter c

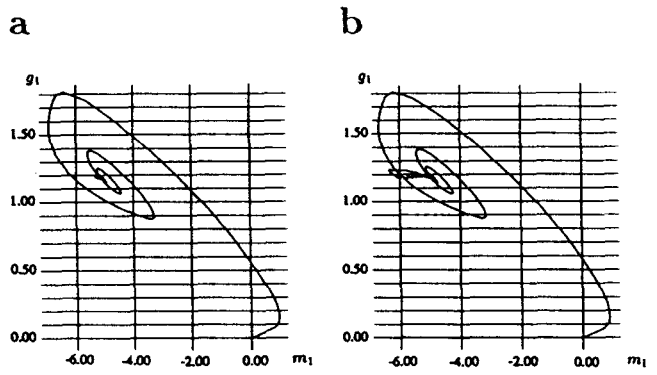

Fig. 6a, b. Bifurcation from fixed point to finite amplitude oscillation. **a** $c = -2.60$; **b** $c = -2.52$

For negative values of c, the bifurcation between the regions VI and VII has already been mentioned. The bifurcation between the regions VII and VIII was different in that the limit cycle had a finite amplitude at the bifurcation point (Fig. 6).

4.2 Synaptic modification-induced transition

After determining different attractor regions in terms of lateral connection strengths, it was natural to ask how synaptic modification can induce transitions between these regions. It was expected that slowly varying the synaptic strengths could result in dramatic and instantaneous changes of the qualitative dynamic behaviour. A learning process materializes synaptic modifications. Specifically, transitions between oscillatory and chaotic states due to learning have been suggested (Skarda and Freeman 1987). It was assumed in the simulations presented here that only the lateral excitatory connections between mitral cells could be modified, though there is evidence (Brennan et al. 1990) for the modifiability of the dendro–dendritic mitral–granule synapses as well.

4.2.1 Formalization of the problem. The set (2) of ODEs was supplemented with differential equations for the matrix elements L_{ij}. The increase of synaptic strengths can easily be formalized using Hebb's (1949) rule:

$$\dot{L}_{ij}(t) = k \cdot \phi_m(m_i(t)) \cdot \phi_m(m_j(t)) , \qquad (4)$$

where the constant k controls the rate of learning. Only nearest neighbour connections were taken into account here, i.e. $j = i - 1$ or $j = i + 1$.

The randomly chosen vector elements I_i^{rec} (as in Sect. 4.1) ensured that the values $m_i(t)$ were different for different i's, thus different matrix elements L_{ij} were also modified differently.

The initial state $L(0)$ determined the attractor region where the learning process started. To study the transition between two physiologically plausible attractors, from oscillations to chaos, region II in Fig. 2 was chosen as starting point.

4.2.2 Simulation results. In this series of simulations, $c = 1$ was chosen for convenience. Thus the uniform initial values $L_{ij}(0) = 0.3$ for all neighbours i, j corresponded to the state $c = 0.3$ of the previous section which was inside the periodic region II of Fig. 2. The value $k = 0.015$ of the learning rate was found to be sufficiently large to induce transition to region III within a reasonable time and sufficiently small not to destroy the patterns obtained without learning. The values of all other parameters were set as previously (see Appendix).

Since the phase space technique cannot be applied to temporally changing qualitative dynamics, the output of one mitral cell versus time was directly plotted here, and the average inward synaptic strength was also monitored supplementing the time scale. Figure 7a shows the full learning process. In the early phase of learning (Fig. 7b), the amplitude of the oscillation of the periodic region II gradually increased. Later (right-hand side of Fig. 7b) the period doubling could be observed. After an intermediate multiperiodic stage, Fig. 7c shows the emergence of chaos. Learning was stopped when the average synaptic strength reached 0.4, which was inside the chaotic region III.

The oscillations of all neurons remained synchronized even in the multiperiodic stage, and the transitions also happened simultaneously, although the rate of synaptic modification was different from cell to cell due to the randomly chosen input. This result shows that the inherent synchronous activity was a robust property of the model.

4.3 Associative memory: recognition of incomplete odour patterns

The problem of associative memory is a particularly difficult issue in sensory systems where continuous interaction with the environment is explicitly taken into account. The task to be solved here is a special case of odour recognition with a time-continuous input.

Our aim was to show that incomplete input patterns due to lower odour concentration could also be identified as proper stimuli if a suitable learning rule was used to modify the lateral connections between mitral cells. A further difficulty of this approach was the existence of very restrictive additional constraints on the periodic temporal patterns that emerged when the odour input was present.

4.3.1 Formalization of the problem. An odour pattern was denoted by the vector $\mathbf{P} = \{P_1, P_2, \ldots, P_N\}$ with P_i being 0 or 1. The size of the pattern, i.e. the number of active cells in it, was taken as the squared length of the vector $\mathbf{P}$. A vector $\mathbf{p}$ was called an *incomplete part* of the pattern $\mathbf{P}$ if $p_i \leqslant P_i$ for all i.

The odour input $I^{\text{odour}}(t)$ was only given to the active cells of the input pattern, while other cells only received the constant background input I^{backgr}. $I^{\text{odour}}(t)$ followed the sniff cycle and carried a sequence $s = 1, 2, \ldots$ of different incomplete parts $\mathbf{p}^{(s)}$ of the odour pattern $\mathbf{P}$. The linear increase and the exponential decrease during the period ($T = 400$ ms) of one sniff

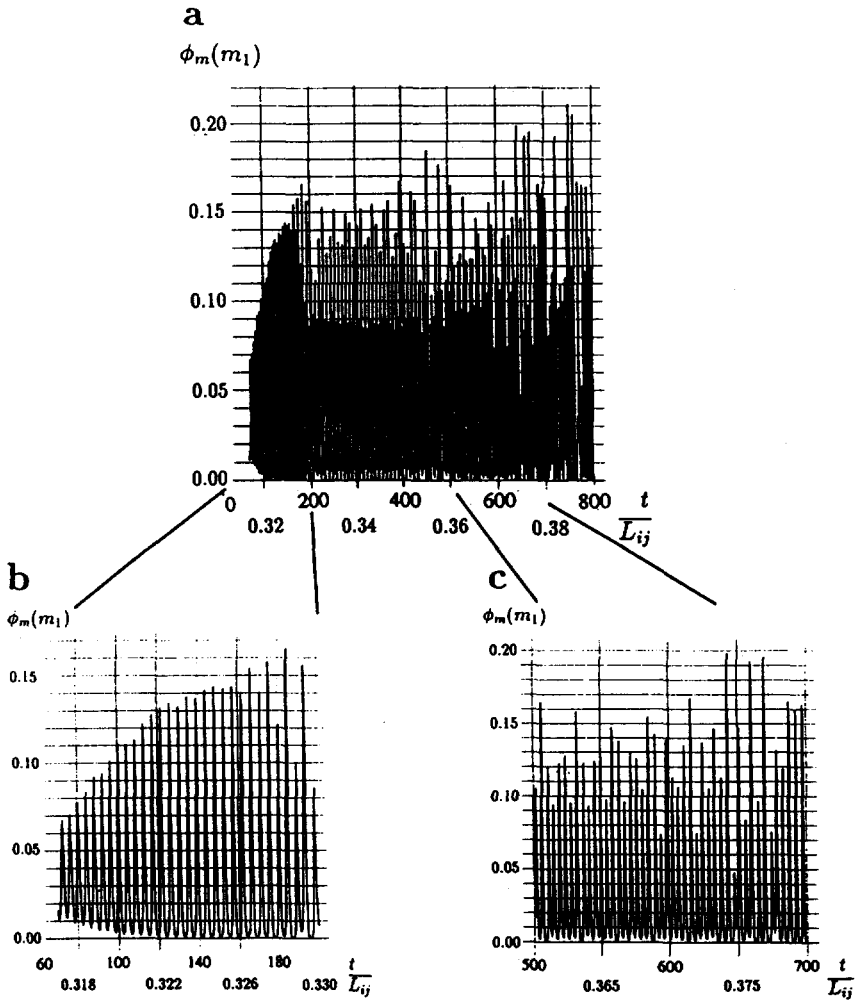

Fig. 7a–c. Synaptic modification induced bifurcation. Both the time scales and the corresponding values of the average lateral synaptic strengths are indicated on the horizontal axis. Vertical axis: output of an arbitrarily chosen mitral cell. **a** The full learning process; **b** oscillation and period doubling at the beginning of the process; **c** the emergence of chaos at the end of the process

cycle was adopted from Li and Hopfield (1989):

$$I_i^{\text{odour}}(t) = \begin{cases} p_i^{(s)} \cdot (t - t^{\text{inh}})/(t^{\text{exh}} - t^{\text{inh}}) & \text{if } t^{\text{inh}} \leqslant t < t^{\text{exh}} \\ p_i^{(s)} \cdot \exp\left(-\dfrac{1}{\tau}(t - t^{\text{exh}})\right) & \text{if } t \geqslant t^{\text{exh}}, \end{cases} \quad (5)$$

where $p_i^{(s)}$ is 0 or 1, t^{inh} and t^{exh} are the onset times for inhalation and exhalation, respectively, and τ is the exhalation time constant.

The lateral connection matrix L was fully interconnected here, but self-excitation was excluded, i.e. $L_{ij} > 0$ if $i \neq j$ and $L_{ii} = 0$ for all i. The learning rule consists of three terms. First, a second-order decay term controls the upper bound of the increase of connection strengths. A similar non-linear forgetting term has been introduced by Riedel and Schild (1992). Second, a Hebbian term is responsible for the strengthening of connections between simultaneously firing cells. Finally, the third term is introduced to selectively decrease the synaptic strength between active and inactive cells:

$$\dot{L}_{ij}(t) = -k_1 \cdot L_{ij}^2(t) + k_2 \cdot \phi_m(m_i(t)) \cdot \phi_m(m_j(t)) - \\ - k_3 \cdot L_{ij}(t) \cdot [\phi_m(m_i(t)) - \phi_m(m_j(t))]^2, \quad (6)$$

where k_1, k_2, k_3 are positive constants. The (6) learning rule is local, i.e. the change of a synaptic weight only depends on its value and the activity of the pre- and postsynaptic neurons. The learning task was to modify the initially randomly distributed synaptic weights so that the incomplete input patterns $\mathbf{p}^{(s)}$ evoked the mitral response characteristic to the odour pattern $\mathbf{P}$.

4.3.2 Simulation results. The initial values $L_{ij}(0)$ of the synaptic strengths were taken from the Gaussian distribution $\mathcal{N}(0.12, 0.06)$. The values of the learning constants are given in the Appendix. The time was scaled so that with $T = 400$ ms the average spike frequency was 40–60 Hz. During learning, the different incomplete parts of the same odour pattern were presented randomly. The specifically constructed learning rule with proper parameter values ensured the separation of synaptic weights without violating their boundedness and sign-preserving property. The decreasing connection strengths converged to zero, whereas the increasing ones remained between 0.15 and 0.25 in the long run, thus there was no need to "switch off" the learning process.

Figure 8 shows the outputs of the 11 mitral cells during one sniff cycle before learning (a) and after 60

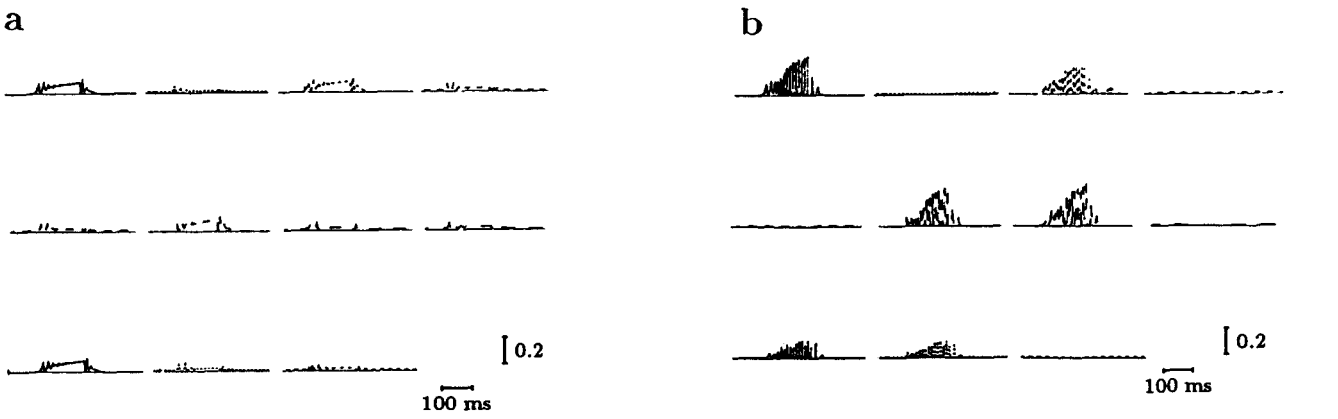

Fig. 8. Outputs of the $N = 11$ mitral cells **a** before and **b** after learning. The incomplete patterns (1 0 1 0 0 1 0 0 1 0 0) and (1 0 1 0 0 1 1 0 1 1 0), respectively, were presented as input. The complete odour pattern was (1 0 1 0 0 1 1 0 1 1 0)

cycles of learning (b). Before learning, only the four cells that received the incomplete input pattern produced relevant but still very low output because the weak lateral connections did not transmit their low activities to the other cells. In contrast, Fig. 8b shows that all six cells belonging to the complete odour pattern exhibited large-amplitude, high-frequency firing bursts, although only four of them received the odour input. The oscillations of different cells were synchronized, with a frequency around 60 Hz. It can be concluded that the learning rule (6) leads to the recognition of incomplete odour patterns, preserving physiologically justified oscillatory burst activities (see Li and Hopfield 1989) at the same time.

5 Discussion

The modelling of information processing in the OB is one of the newest "work-horses" in the realm of real neural network models. In this paper, a two-level neurodynamic model has been defined and studied numerically to describe the activity patterns and synaptic modifiability. Preliminary results have been published elsewhere (Érdi et al. 1992; Grőbler et al. 1992).

The architecture of the network was constructed by focusing on the nature of the mitral–granule cell interactions. A further step in model building would be to take into account the glomerular fine structure of mitral cell dendrites as well (Schild and Riedel 1992).

The effects of both lateral inhibition and excitation in the mitral layer on the dynamic behaviour have been studied. The nature of the attractors and also the bifurcation sequences were determined. The results of computer simulations have shown that chaotic activity can only be found if lateral excitation is assumed. In spite of efforts made recently (e.g. Skarda and Freeman 1987; Yao and Freeman 1990), the functional role of chaotic behaviour in the OB has not yet been entirely clarified.

Lateral interactions have special importance in the model. A transition from the oscillatory to the chaotic region by the continuous-time modification of lateral synaptic strengths was studied by adopting a moderately slow learning process.

Synaptic modifiability is closely associated with learning and memory. The associative memory character of the OB was modelled by explicitly taking into account the continuous nature of the sensory input and of the learning process. The simulation results are in accordance with the ideas proposed by Hudson et al. (1990), who suggested that even small and rather arbitrary regions of the OB are capable of odour processing, and that olfactory information processing has a distributive character.

The OB is the first relay centre of the olfactory system. Several publications have dealt with modelling of the next stage of olfactory information processing, namely the olfactory cortex (Granger et al. 1989; Barnard 1989; Ambros-Ingerson et al. 1990; Hopfield 1991; Liljenström 1991; Wilson and Bower 1992) and even with bulbo-cortical and cortico-bulbar connections (Bressler 1987a,b). Since the olfactory cortex itself generates intrinsic oscillation, a unified model should exhibit highly complex activity patterns and should also explain short-term and long-term memory phenomena.

Acknowledgements. We thank Robyn Hudson and Hans Distel for motivating us to study the olfactory system. Parts of this work have been discussed with Kaisa Hartikainen, Hans Liljenström, and Henrik Farkas. Conversations with Walter Freeman, Detlev Schild and Ichiro Tsuda were very useful. This research was supported by the Academy of Finland, the Japan Society for Promotion of Sciences JSPS (to GB) and the National Scientific Research Fund (Hungary) under grant number OTKA 1821 (to PÉ).

Appendix:

List of parameter values

Parameter	Description	Value		
		Sect. 4.1	Sect. 4.2	Sect. 4.3
N	Number of mitral (granule) cells	11	11	11
S'_m	Mitral transfer function parameter	0.14	0.14	0.14
S_m	Mitral transfer function parameter	1.4	1.4	1.4
S'_g	Granule transfer function parameter	0.29	0.29	0.29
S_g	Granule transfer function parameter	2.9	2.9	2.9
θ	Transfer function threshold	1.0	1.0	1.0
a	Decay constant for mitral cells	0.1	0.1	0.1
b	Granule-to-mitral coupling constant	1.0	1.0	1.0
c	Mitral-to-mitral coupling constant	−5.0–5.0	1.0	1.0
d	Decay constant for granule cells	0.2	0.2	0.2
e	Mitral-to-granule coupling constant	1.2	1.2	1.2
α	Odour input scaling constant	1.0	1.0	0.32
I^{odour}	Odour input	1.0[a]	1.0[a]	—[b]
I^{backgr}	Receptor background input	0	0	0.02
I^{cort}	Cortical input to granule cells	0.1	0.1	0.1
M_{ij}	Mitral-to-granule connection matrix			
	$i=j$	1.0	1.0	1.0
	$\lvert i-j\rvert=1$	0.5	0.5	0.5
	$\lvert i-j\rvert>1$	0	0	0
G_{ij}	Granule-to-mitral connection matrix			
	$i=j$	1.0	1.0	1.0
	$\lvert i-j\rvert=1$	0.5	0.5	0.5
	$\lvert i-j\rvert>1$	0	0	0
L_{ij}	Mitral-to-mitral connection matrix			
	$i=j$	0	0	0
	$\lvert i-j\rvert=1$	1.0	—[b]	—[b]
	$\lvert i-j\rvert>1$	0	0	—[b]
k	Learning constant in eq. (4)	—	0.015	—
T	Period of sniff cycle	—	—	400 ms
τ	Exhalation time constant	—	—	33 ms
k_1	Learning constant in eq. (6)	—	—	10^{-5}
k_2	Learning constant in eq. (6)	—	—	0.1
k_3	Learning constant in eq. (6)	—	—	0.1
$\mathbf{P}^2$	Size of complete odour pattern	—	—	6
$\mathbf{p}^2$	Size of incomplete input patterns	—	—	4

[a] Expectation of a Gaussian distribution
[b] The parameter is a function of time (see text for details)

References

Adrian ED (1950) The electrical activity of the mammalian olfactory bulb. Electroencephalogr Clin Neurophysiol 2:377–388

Ambros-Ingerson L, Granger R, Lynch G (1990) Simulation of paleocortex performs hierarchical clustering. Science 247:1344–1348

Baird B (1986) Non-linear dynamics of pattern formation and pattern recognition in the rabbit olfactory bulb. Physica 22D:150–179

Baird B (1990) Bifurcation and category learning in network models of oscillating cortex. Physica 42D:365–384

Barnard E (1989) Analysis of the Lynch–Granger model for olfactory cortex. Biol Cybern 62:151–155

Brennan P, Keverne EB (1989) Impairment of olfactory memory by local infusions of non-selective excitatory amino acid receptor antagonists into the accessory olfactory bulb. Neuroscience 33:463–468

Brennan P, Kaba H, Keverne EB (1990) Olfactory recognition: a simple memory system. Science 250:1223–1226

Borisyuk RM, Kirillov AB (1992) Bifurcation analysis of a neural network model. Biol Cybern 66:319–325

Bressler SL (1987a) Relation of olfactory bulb and cortex. I. Spatial variation of bulbo-cortical interdependence. Brain Res 409:285–293

Bressler SL (1987b) Relation of olfactory bulb and cortex. II. Model for driving of cortex by bulb. Brain Res 409:294–301

Érdi P, Grőbler T, Kaski K (1992) Dynamic phenomena in the olfactory bulb. I. Bifurcation sequences, coexistence of periodicity and chaos, synaptic modification induced transitions. In: Aleksander I, Taylor J (eds) Artificial neural networks 2. North-Holland, Amsterdam, pp 873–876

Freeman WJ (1975) Mass action in the nervous system. Academic Press, New York

Freeman WJ (1978) Spatial properties of an EEG event in the olfactory bulb and cortex. Electroencephalogr Clin Neurophysiol 44:585–605

Freeman WJ (1979) Nonlinear gain mediating cortical stimulus-response relations. Biol Cybern 33:237–247

Freeman WJ, Schneider W (1982) Changes in spatial patterns of rabbit olfactory EEG with conditioning to odours. Psychophysiology 19:44–56

Freeman WJ, Skarda C (1985) Spatial EEG patterns, non-linear dynamics and perception: the neo-Sherringtonian view. Brain Res Rev 10:147–175

Frouzakis CE, Adomaltis RA, Kevrekidis IG (1991) Resonance phenomena in an adaptively controlled system. Int J Bifurcation Chaos 1:83

Granger R, Ambros-Ingerson J, Lynch G (1989) Derivation of

encoding characteristics of layer II cerebral cortex. J Cog Neurosci 1:61–87
Grőbler T, Érdi P, Kaski K (1992) Dynamic phenomena in the olfactory bulb. II. Model for a simple associative memory. In: Aleksander I, Taylor J (eds) Artificial neural networks 2. North-Holland, pp 877–880
Halász N (1990) The vertebrate olfactory system. Akadémiai Kiadó, Budapest
Hebb DO (1949) The organization of behaviour. Wiley, New York
Holley A (1991) Neural coding of olfactory information. In: Getchell TV et al (eds) Smell and taste in health and disease. Raven Press, New York, pp 329–343
Hopfield JJ (1991) Olfactory computation and object perception. Proc Natl Acad Sci USA 88:6462–6466
Hudson R, Distel H (1987) Regional autonomy in the peripheral processing of odour signals in newborn rabbits. Brain Res 421:85–94
Hudson R, Distel H, Zippel P (1990) Perceptual performance in peripherically reduced olfactory systems. In: Schild D (ed) Chemosensory information processing. Springer, Berlin Heidelberg New York, pp 259–279
Keener (1981) Infinite period bifurcation and global bifurcation branches. SIAM J Appl Math 41:127–144
Li Z (1990) A model of olfactory adaptation and sensitivity enhancement in the olfactory bulb. Biol Cybern 62:349–361
Li Z, Hopfield JJ (1989) Modelling the olfactory bulb and its neural oscillatory processings. Biol Cybern 61:379–392
Liljenström H (1991) Modelling the dynamics of olfactory cortex using simplified network units and realistic architecture. Int J Neural Systems 2:1–15
Riedel H, Schild D (1992) The dynamics of Hebbian synapses can be stabilized by a nonlinear decay term. Neural Networks 5:454–463
Schild D (1988) Principles of odour coding and a neural network for odour discrimination. Biophys J 54:1001–1011
Schild D (1990) Chemosensory information processing. (NATA ASI Series vol H 39) Springer, Berlin Heidelberg New York
Schild D, Riedel H (1992) The significance of glomerular compartmentalization for olfactory coding. Biophys J 61:704–715
Scott JW (1991) Central processing of olfaction. J Steroid Biochem Biol 39:593–600
Scott JW, Harrison TA (1987) The olfactory bulb: anatomy and physiology. In: Finger TE, Silver WL (eds) Neurobiology of taste and smell. Wiley, New York
Shepherd GM, Greer CA (1990) Olfactory bulb. In: Shepherd GM (ed) The synaptic organization of the brain. Oxford University Press, New York, pp 133–169
Skarda C, Freeman WJ (1987) How brains make chaos in order to make sense of the world. Behav Brain Sci 10:161–195
Taylor JG, Keverne BE (1991) Accessory olfactory learning. Biol Cybern 64:301–305
Trombley PO, Shepherd GM (1991) Norepinephrine inhibits mitral cell evoked EPSPs in mammalian olfactory bulb granule cells in culture. Soc Neurosci Abstr 17:103–12
Willey TJ (1973) The ultrastructure of the cat olfactory bulb. J Comp Neurol 152:211–232
Wilson MA, Bower JM (1992) Cortical oscillations and temporal interactions in a computer simulation of piriform cortex. J Neurophysiol 67:981–995
Yao Y, Freeman WJ (1990) Model of biological pattern recognition with spatially chaotic dynamics. Neural Networks 3:153–170